2010

Crystal field effects on the reactivity of aluminum-copper cluster anions

Patrick J. Roach
Pennsylvania State University - Main Campus

W. Hunter Woodward
Pennsylvania State University - Main Campus

Arthur C. Reber
Virginia Commonwealth University

Shiv N. Khanna
Virginia Commonwealth University, snkhanna@vcu.edu

A. W. Castleman Jr.
Pennsylvania State University - Main Campus

Crystal field effects on the reactivity of aluminum-copper cluster anions

Patrick J. Roach,[1] W. Hunter Woodward,[1] Arthur C. Reber,[2] Shiv N. Khanna,[2,*] and A. W. Castleman, Jr.[1,†]

[1]*Departments of Chemistry and Physics, The Pennsylvania State University, University Park, Pennsylvania 16802, USA*

[2]*Department of Physics, Virginia Commonwealth University, Richmond, Virginia 23284, USA*

The limits and useful modifications of the jellium model are of great interest in understanding the properties of metallic clusters, especially involving bimetallic systems. We have measured the relative reactivity of $CuAl_n^-$ clusters ($n=11-34$) with O_2. An odd-even alternation is observed that is in accordance with spin-dependant etching, and $CuAl_{22}^-$ is observed as a "magic peak." The etching resistance of $CuAl_{22}^-$ is explained by an unusually large splitting of the $2D^{10}$ subshell that occurs because of a geometric distortion of the cluster that may also be understood as a crystal field splitting of the superatomic orbitals.

PACS number(s): 36.40.Cg, 36.40.Jn, 36.40.Wa

I. INTRODUCTION

A generalized understanding of the electronic structure of metal clusters is desirable to aid efforts to integrate clusters into materials and catalysts.[1,2] The electronic structure of simple-metal clusters in the gas phase is known to agree with the predictions of a jellium electronic shell model, which uses the confined nearly free electron picture and considers the ionic cores as a uniform positive background.[3,4] The shape of the potential well that confines the free electrons is defined by the arrangement and identity of the atoms within the cluster, with solutions of the Schrödinger equation yielding discrete electronic energy levels.[3] Gaps in the energies of electronic levels are considered to be subshell closings. In spherical clusters, subshell closings occur at electron counts of $n^*=2, 8, 18, 20, 34, 40, 58, 68, 70,\ldots$ electrons, corresponding to 1S, 1P, 1D, 2S, 1F, 2P, 1G, 2D, 3S… subshells, respectively.

The reduced reactivity of specific aluminum clusters with molecular oxygen is well known to occur in species with closed jellium electronic shells.[5] The conservation of electronic spin angular momentum and the triplet ground state of O_2 is responsible for this relationship.[6–8] Spin conservation requires that the aluminum cluster accommodate the excess spin of O_2 for an etching reaction to occur. We have previously[7] proposed that a quasistatically approximated quantity, which we refer to as the vertical spin excitation energy (VSE), is appropriate for predicting or explaining the reactivity of an aluminum containing cluster with oxygen. The VSE of a cluster with a singlet ground state is calculated as the energy difference of the ground state geometry with singlet and triplet spin multiplicities. The VSE is related to the HOMO-LUMO gap in singlet clusters. Doublet species, with an unpaired electron, all etch quickly because the spins can pair in either direction. Therefore, a singlet cluster with a large HOMO-LUMO gap is expected to show a resistance to oxygen etching with respect to other clusters having smaller HOMO-LUMO gaps.

Clusters with electron counts that result in partially filled electronic shells are susceptible to Jahn-Teller distortions, which can result in significant splitting in levels which are predicted to be degenerate in the spherical shell model.[9–13] A spheroidal shell model was proposed to explain the influence of prolate and oblate distortions in alkali-metal atomic clusters.[10] It has also been shown that reducing the symmetry from the ideal R_3 group to I_h breaks the degeneracy within the 1F and 1G subshells.[14–16] Recently, the energetic differentiation of the states within the same electronic subshell was observed experimentally by velocity map imaging photo electron spectroscopy.[17] We show here that an analysis of the crystal field splitting of the 2D subshell levels can be used to intuitively explain the electronic structure of $CuAl_{22}^-$ that results in its reduced reactivity with O_2.

Section II presents the details of the experimental method while Sec. III provides details on the theoretical approach. Section IV presents the experimental and theoretical findings, and Sec. V contains a discussion of the results. Section VI concludes our findings.

II. EXPERIMENTAL METHODS

The reactivity of $CuAl_n^-$ clusters ($n=11-34$) with O_2 was measured using a fast-flow reactor mass spectrometer system that has been described in detail previously.[18,19] Briefly, clusters were generated in the restricted volume of a laser vaporization (LaVa) source by impinging a pulsed Nd:YAG laser (532 nm) upon the surface of a rotating/translating aluminum alloy rod with a high copper content (McMaster-Carr, 2000 series alloy) in the presence of a continuous flow (8000 standard cubic centimeters per minute of helium carrier gas). Clusters created in the source were entrained in a high pressure helium stream and injected into the reaction tube. The reactor was maintained at ~0.7 Torr with a high-volume Roots blower where the clusters were cooled to room temperature and allowed to react with the O_2 reactant gas. Mass analysis of the initial and reaction products was performed using a custom-built mass spectrometer, (designed and constructed in collaboration with Extrel CMS), which incorporates a quadrupole filter for mass analysis (Extrel, 150-QC) and a computer interface (Merlin Automation) for the acquisition of mass spectra.

III. THEORETICAL METHODS

The structural geometries, one electron orbitals, and Eigenstates of $CuAl_n^-$ clusters ($n=11-22$) were calculated

using a linear combination of Gaussian orbitals molecular orbital approach within a density functional theory (DFT) formalism. Calculations were performed using NRLMOL code[20–22] with a gradient corrected PBE functional.[23] Basis sets consisting of six S, five P, and four D Gaussians for Al, and seven S, five P, and four D Gaussians for Cu were employed. Molecular orbitals were assigned subshell distinctions based on the symmetry group of the molecular orbitals whenever possible, and through inspection of the nodes in the calculated wave functions. We would like to add that the above analysis allowed a fairly clear assignment of the orbitals in all undistorted cases allowing a correspondence to the orbitals in the nearly free electron jellium model. For each size, 20 to 50 geometries were optimized without constraint starting with known isomers for pure aluminum clusters and isomers produced by a genetic algorithm which used Gupta potentials.[24] To validate our method, we calculated the vertical detachment energy for $CuAl_{12}^-$, and compared our result with the available photodetachment spectra measured by Wang and co-workers.[25] We calculated a detachment energy of 3.14 eV from the singlet $CuAl_{12}^-$ to doublet $CuAl_{12}$ while previous theory and experiment give 3.15 and 3.31 eV respectively, showing good agreement.

IV. RESULTS

The experimental mass spectra of $CuAl_n^-$ clusters ($n=11-34$) are presented in Fig. 1. The nascent cluster distribution [Fig. 1(a)] consists of a smoothly varying envelope of cool Al_n^- and $CuAl_n^-$ clusters.[26] To discriminate $CuAl_n^-$, spectra of the nascent [Fig. 1(b)] and reacted [Fig. 1(c)] distributions from Al_n^-, which are simultaneously present in this experiment, the presented spectra were modified by the removal of peaks corresponding to Al_n^-. The unmodified spectra is available in Fig. S1.

Significant deviations in the intensity of peaks in the $CuAl_n^-$ distribution are observed upon addition of the O_2 reactant gas. Species corresponding to $CuAl_n^-$ ($n=$odd) react completely away, whereas many species corresponding to $CuAl_n^-$ ($n=$even) remain with differing intensities. $CuAl_n^-$ ($n=16$ and 28) are conspicuously absent from the ($n=$even) distribution. $CuAl_{12}^-$ is also not observed in the reacted distribution, though the absence of any smaller clusters prevents the elimination of mass discrimination effects of the flow reactor extraction optics for this particular cluster, when determining the reactivity. The species $CuAl_{22}^-$ is observed as the largest peak in the product spectrum of this binary metallic series, and we consider it as a "magic" peak.

The low lying isomers of $CuAl_{22}^-$ based on theoretical investigations are shown in Fig. 2. The atomic coordinates of the lowest energy isomer [Fig. 2(a)] are distinctly similar to the recently reported lowest energy structure of Al_{23}^+, which has a similar HOMO-LUMO gap of 1.19 eV and is isoelectronic.[27] The magnitude of vertical spin excitation energies (VSE) of $CuAl_n^-$ are plotted in Fig. 3. The calculated VSEs of the $n=$even clusters show a nearly exact coincidence with the peak intensities in the product spectrum [Fig. 1(c)]. The agreement provides further support for spin-dependant oxygen etching, and further attests to the propriety
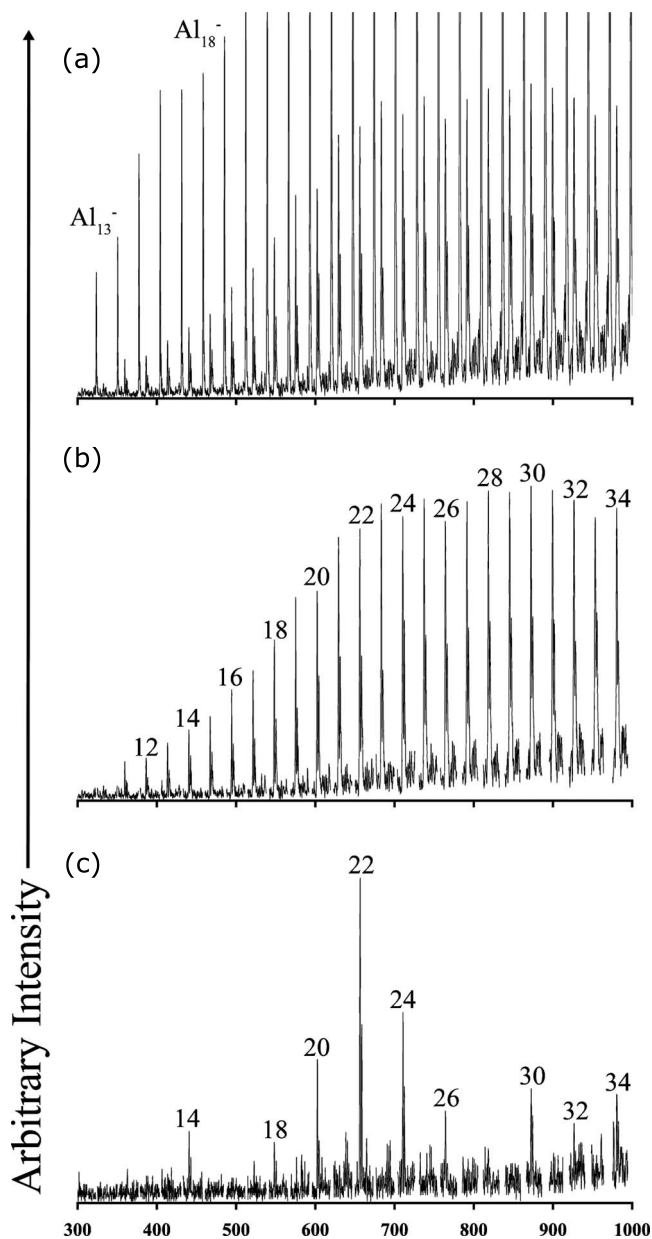

FIG. 1. (a) Nascent distribution of Al_n^- and $CuAl_n^-$. (b) Nascent $CuAl_n^-$ distribution (c) Oxygen-etched $CuAl_n^-$ distribution (1.25% partial pressure of oxygen). Peaks corresponding to pure aluminum clusters were superficially removed from (b) and (c) to discriminate $CuAl_n^-$.

of using a calculated vertical spin excitation as a metric for determining oxygen reactivity.

V. DISCUSSION

While the resistance of $CuAl_{22}^-$ to oxygen etching is reasonably explained by its relatively large VSE, we wish to discuss why its VSE and HOMO-LUMO gap is larger than that of the other species. The size of the HOMO-LUMO gap is closely related to the VSE of a cluster, as the spin exchange energy is small.[7] The HOMO-LUMO gap of a metal cluster with a complete jellium electronic subshell is ex-
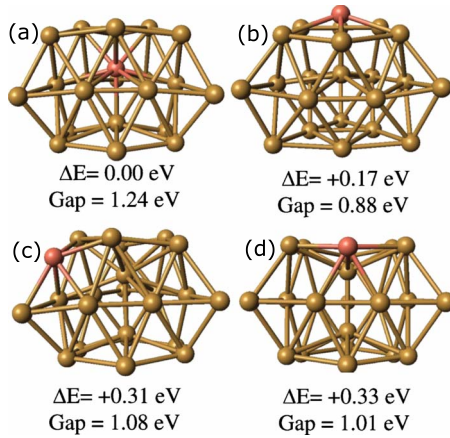
FIG. 2. (Color online) (a)–(d) Lowest energy structures and HOMO-LUMO gap (Gap) for $^1CuAl_{22}$. ΔE is the relative energy of the structures with respect to the ground state.

pected to be large. One possible explanation for the reactive resistance of $CuAl_{22}$, which we ultimately will argue against, might be that the species $CuAl_{22}^-$ is a closed shell jellium species.

For the purpose of a shell model analysis, we consider $CuAl_{22}^-$ to have 68 itinerant valence electrons. Each aluminum atom contributes three sp hybridized electrons ($3 \times 22 = 66$), the copper atom donates its $4s^1$ electron ($66 + 1 = 67$), and an additional electron is counted for the anion ($67 + 1 = 68$).[27,28] The localized $3d$ electrons of copper are excluded, just as they have been in similar analyses.[29,30] Figure S2 shows the projected density of states for the Cu (s) states, and shows that the atomic state is extensively hybridized into the delocalized cluster states.

In the spherical shell model, 68 electrons correspond to a closed $2D^{10}$ shell, with an empty $3S^2$. A previous analysis suggested that within a spherical approximation, the cluster $CuAl_{22}^-$ would only have a closed subshell if the copper atom resided at an external position of the cluster.[29] This analysis employed the predictions of a two-level model,[31] which accounts for stabilization of the orbitals with lower angular momentum when a more electronegative atom is positioned at a central position in the background potential. Such central positioning of the copper atom in the cluster $CuAl_{22}$ would
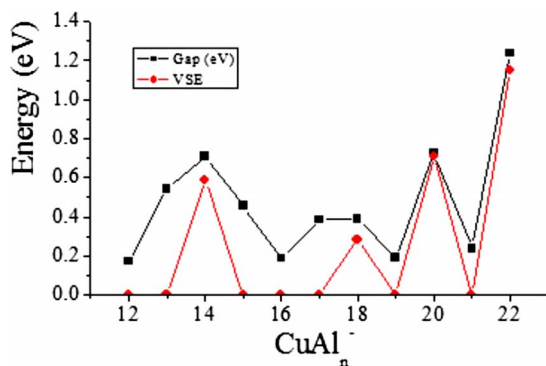

FIG. 3. (Color online) Calculated HOMO-LUMO Gap and vertical spin excitation energy (VSE) of the $CuAl_n^-$ clusters. See Fig. S3 and S4 for structural information.
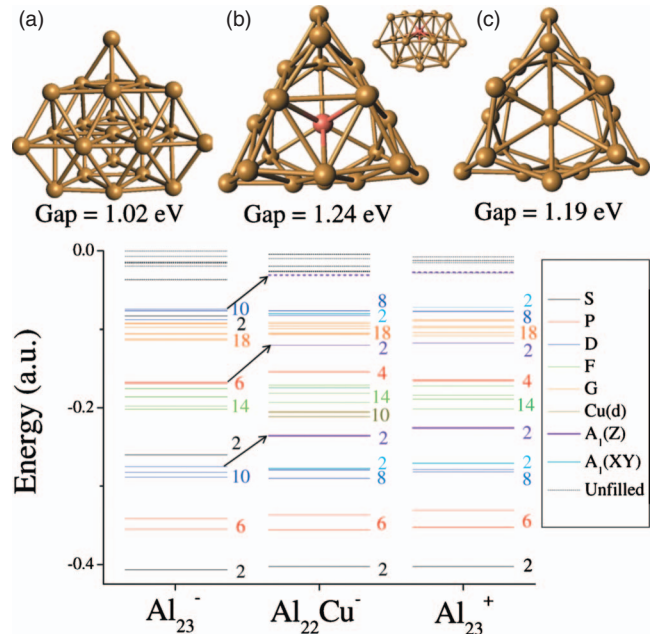

FIG. 4. (Color) Geometry and HOMO-LUMO Gaps of (a) Al_{23}^-, (b) $CuAl_{22}^-$, and (c) Al_{23}^+. Below, the electronic structure of (a), (b), and (c) with labeled shells. $A_1(XY)$ and $A_1(Z)$ indicate hybridized levels with extra nodes along the XY and Z planes.

be expected to result in the stabilization of the $3S^2$ states, resulting in a disappearance of the closed subshell at 68 electrons that is predicted by the spherical shell model. However, the lowest energy structure of $CuAl_{22}^-$ [Fig. 2(a)], along with most previous work on $CuAl_n^-$ clusters[25,29–32] has the copper atom located at a central position, and moreover is not well approximated by a sphere.

The calculated electronic structures of Al_{23}^- and $CuAl_{22}^-$ are shown in Fig. 4. Al_{23}^- has 70 itinerant electrons, a HOMO-LUMO gap of 1.02 eV and is reasonably approximated by a sphere. The calculated electronic structures of both species (Fig. 4) have discernible gaps that we interpret as shell structure. The close lying electronic states of Al_{23}^- have distinct jumps in energy at 2, 8, 18, 20, 40, and 70 valence electrons, the HOMO consists of five nearly degenerate 2D orbitals, and inspection of the charge densities confirm that the $2D^{10}$ subshell is higher in energy than the $3S^2$ subshell. This is consistent with the subshell ordering of $1S^2|1P^6|1d^{10}2S^2|1F^{14}2P^6|1G^{18}3S^22D^{10}|1H^{22}$, wherein the observed gaps are denoted by vertical lines. The observed gaps are also consistent with the predictions of Cheng $et\ al.$[13] In $CuAl_{22}^-$, the levels rearrange and now have jumps in energy at 2, 8, 18, 20, 38, and 68 valence electrons. The observed gap counts could be obtained by rearranging the subshells such that they are ordered as $1S^2|1P^6|1D^{10}2S^2|1G^{18}|1F^{14}2P^6|2D^{10}|3S^2$. While there is precedent for the rearrangement of subshells in centrally doped clusters,[29] there is no readily available explanation for the haphazard movement of the 1G shell that is required in the above reordering. Additionally, the level structure of Al_{23}^+, shown in Fig. 4, is nearly identical to that of $CuAl_{22}^-$, except for the atomic $3d$-shell electrons of copper, further suggesting that a subshell rearrangement is not an appropri-
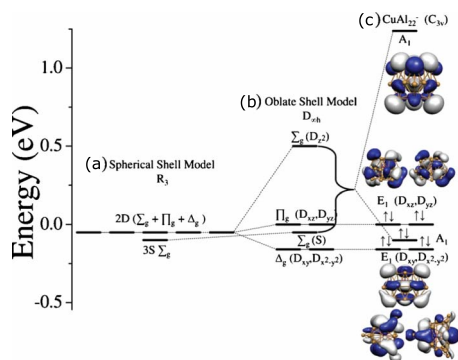
FIG. 5. (Color online) (a) 2D and 3S spherical shell levels. (b) Predicted crystal field splitting caused by negative point charges placed on opposite sides of the cluster along the Z axis, and (c) the calculated splitting in $CuAl_{22}^-$ using DFT.

ate explanation for the observed shell closings. Without reordering the subshells from the structure of Al_{23}^-, gaps must occur between within the 2P and 2D subshells, such that the electronic structure can be drawn as $1S^2|1P^6|1D^{10}2S^2|1F^{14}2P^4|2P^21G^{18}3S^22D^8|2D^21H^{22}$. However, justification for the splitting of subshells is required.

The lowest energy structure of $CuAl_{22}^-$, shown in Fig. 3(a) can be described as an oblate structure with decreased height along the z axis relative to the width along the xy plane. The effect of an oblate distortion on the electronic shell structure of $CuAl_{22}^-$ may be qualitatively predicted[13–16,33–35] using concepts from crystal field theory, in which the ions of the cluster generate a crystal field which affects the confined nearly free electron gas. As shown in Fig. 5, the electronic structure of a spherical jellium cluster, analogous to the electronic structure of Al_{23}^- [Fig. 5(a)], would undergo an expected crystal field type splitting [Fig. 5(b)] in which D_{xy}, and $D_{x^2-y^2}$ would be degenerate and lowest in energy, D_{xz} and D_{yz} would be degenerate and of intermediate energy, and D_{z^2} would be highest in energy. While the splitting of the electronic levels is caused by the distorted position of the ionic cores, this splitting may be more easily visualized by considering the modification of the electronic structure due to a pair of negative point charges on opposite sides of the cluster along the z axis. The $3S^2$ state would be expected to be only weakly affected by the field as it has lower angular momentum and a larger portion of its probability density resides at the center of the structure. The frontier electronic structure of $CuAl_{22}^-$ [Fig. 5(c)] compares favorably with the predicted crystal field splitting [Fig. 5(b)]. Therefore the splitting of the $2D^{10}$ subshell into $2D^8|2D^2$ could be rationalized as a crystal field splitting of the $2D_{z^2}$ state and the remaining 2D states. This splitting is enhanced by the hybridization of the

$2D_{z^2}$ and $3S^2$ states which result in the new states having more nodes along the Z axis and XY plane, respectively. Similarly, the surprisingly large HOMO-LUMO gaps at 38 electrons which are observed in Al_{13}^+ and $Al_{12}Cs^-$ can be explained by the hybridization and splitting of the $2P_z$ and $1F_{z^3}$ states from the 2P and 1F subshells, in which the $2P_z$ state is pushed up in energy to the next shell, and $1F_{z^3}$ is stabilized through hybridization.[36,37] At lower energies, the $1D_{z^2}$ is pushed up in energy and the $2S^2$ is stabilized, resulting in a pronounced gap at 18 electrons. This is also consistent with the twofold degenerate states below this gap having E_1 irreducible representations and the state above this gap having A_1 symmetry, as shown in Fig. 5.

The etching behavior also shows a relationship between geometric rigidity with respect to dopants and electronic structure. $CuAl_{12}^-$, and $CuAl_{16}^-$, shown in Figs. S3 and S4, are rapidly etched, have unusually small gaps and exhibit only a small deviation in geometry from their icosahedron based pure aluminum clusters. All other copper doped clusters reveal different geometries than their Al_n^- counterpart. The smaller size of the copper atom relative to aluminum results in the enhanced stability of the icosahedrons based structures with copper in the central site. This occurs despite the fact that the electron count suggests the cluster should undergo an oblate distortion. This highlights the conflict between electronic and geometric stability.

VI. CONCLUSIONS

In conclusion, we find that $CuAl_{22}^-$ is resistant to oxygen etching. Its large HOMO-LUMO gap is not due to a spherical electronic subshell closure, but can be explained as a result of its distorted shape. The unusually large HOMO-LUMO gap may be understood qualitatively through consideration of the crystal field splitting of the jellium orbitals, where the energy of the D_{z^2} state is increased. This demonstrates that crystal field theory gives intuition in understanding how the electronic shell structure in metal clusters is affected by Jahn-Teller distortions. The use of crystal field concepts to understand cluster phenomenon further demonstrates that models developed for the understanding atomic concepts may be usefully applied to clusters.[38–41]

*snkhanna@vcu.edu

†awc@psu.edu

[1] A. W. Castleman, Jr. and S. N. Khanna, J. Phys. Chem. C **113**, 2664 (2009).

[2] P. J. Roach, W. H. Woodward, A. W. Castleman, Jr., A. C. Reber, and S. N. Khanna, Science **323**, 492 (2009).

[3] W. Knight, K. Clemenger, W. A. de Heer, W. A. Saunders, M. Y. Chou, and M. L. Cohen, Phys. Rev. Lett. **52**, 2141 (1984).

[4] W. A. de Heer, Rev. Mod. Phys. **65**, 611 (1993).

[5] R. E. Leuchtner, A. C. Harms, and A. W. Castleman, Jr., J. Chem. Phys. **91**, 2753 (1989).

[6] P. J. Roach, A. C. Reber, W. H. Woodward, S. N. Khanna, and A. W. Castleman, Jr., Proc. Natl. Acad. Sci. U.S.A. **104**, 14565 (2007).

[7] A. C. Reber, S. N. Khanna, P. J. Roach, W. H. Woodward, and A. W. Castleman, Jr., J. Am. Chem. Soc. **129**, 16098 (2007).

[8] R. Burgert, H. Schnockel, A. Grubisic, X. Li, S. T. Stokes, K. H. Bowen, G. H. Gantefor, B. Kiran, and P. Jena, Science **319**, 438 (2008).

[9] H. A. Jahn and E. Teller, Proc. R. Soc. London, Ser. A **161**, 220 (1937).

[10] K. Clemenger, Phys. Rev. B **32**, 1359 (1985).

[11] M. Koskinen, P. O. Lippas, and M. Manninen, Z. Phys. D: At., Mol. Clusters **35**, 285 (1995).

[12] S. N. Khanna, B. K. Rao, P. Jena, and J. L. Martins, in *Physics and Chemistry of Small Clusters*, edited by P. Jena, B. K. Rao, and S. N. Khanna (Plenum Press, New York, 1986), pp. 435–438.

[13] T. Höltzl, P. Lievens, T. Veszprémi, and M. T. Nguyen, J. Phys. Chem. C **113**, 21016 (2009).

[14] H.-P. Cheng, R. S. Berry, and R. L. Whetten, Phys. Rev. B **43**, 10647 (1991).

[15] K. E. Schriver, J. L. Persson, E. C. Honea, and R. L. Whetten, Phys. Rev. Lett. **64**, 2539 (1990).

[16] H. Häkkinen, M. Moseler, O. Kostko, N. Morgner, M. A. Hoffman, and B. v. Issendorff, Phys. Rev. Lett. **93**, 093401 (2004).

[17] C. Bartels, C. Hock, J. Huwer, R. Kuhnen, J. Schwöbel, and B. von Issendorf, Science **323**, 1323 (2009).

[18] B. C. Guo, S. Wei, Z. Chen, K. P. Kerns, J. Purnell, S. Buzza, and A. W. Castleman, Jr., J. Chem. Phys. **97**, 5243 (1992).

[19] A. W. Castleman, Jr., K. G. Weil, S. W. Sigsworth, R. E. Leuchtner, and R. G. Keesee, J. Chem. Phys. **86**, 3829 (1987).

[20] M. R. Pederson and K. A. Jackson, Phys. Rev. B **41**, 7453 (1990).

[21] K. Jackson and M. R. Pederson, Phys. Rev. B **42**, 3276 (1990).

[22] D. Porezag and M. R. Pederson, Phys. Rev. A **60**, 2840 (1999).

[23] J. P. Perdew, K. Burke, and M. Ernzerhof, Phys. Rev. Lett. **77**, 3865 (1996).

[24] K. Michaelian, Chem. Phys. Lett. **293**, 202 (1998).

[25] R. Pal, L. F. Cui, S. Bulusu, H. J. Zhai, L. S. Wang, and X. C. Zeng, J. Chem. Phys. **128**, 024305 (2008).

[26] G. Gantefor, K. H. Meiwes-Broer, and H. O. Lutz, Phys. Rev. A **37**, 2716 (1988).

[27] X. Li, H. Wu, X. B. Wang, and L. S. Wang, Phys. Rev. Lett. **81**, 1909 (1998).

[28] A. Aguado and J. M. López, J. Chem. Phys. **130**, 064704 (2009).

[29] B. Cao, A. K. Starace, C. M. Neal, M. F. Jarrold, S. Núñez, J. M. López, and A. Aguado, J. Chem. Phys. **129**, 124709 (2008).

[30] O. C. Thomas, W. Zheng, and K. H. Bowen, Jr., J. Chem. Phys. **114**, 5514 (2001).

[31] E. Janssens, S. Neukermans, and P. Lievens, Curr. Opin. Solid State Mater. Sci. **8**, 185 (2004).

[32] S. N. Khanna, C. Ashman, B. K. Rao, and P. Jena, J. Chem. Phys. **114**, 9792 (2001).

[33] H. Bethe, Ann. Physik **3** (5), 135 (1929).

[34] J. E. Orgel, J. Chem. Phys. **23**, 1004 (1955).

[35] T. H. Upton, J. Chem. Phys. **86**, 7054 (1987).

[36] H. Kim, J. Jung, and Y.-K. Han, ChemPhysChem **10**, 341 (2009).

[37] K. Koyasu, M. Akutsu, J. Atobe, M. Mitsui, and A. Nakajima, Chem. Phys. Lett. **421**, 534 (2006).

[38] D. E. Bergeron, A. W. Castleman, Jr., T. Morisato, and S. N. Khanna, Science **304**, 84 (2004).

[39] D. E. Bergeron, P. J. Roach, A. W. Castleman, Jr., N. O. Jones, and S. N. Khanna, Science **307**, 231 (2005).

[40] M. Walter, J. Akola, O. Lopez-Acevedo, P. D. Jadzinsky, G. Calero, C. J. Ackerson, R. L. Whetten, H. Gonbeck, and H. Hakkinen, Proc. Natl. Acad. Sci. U.S.A. **105**, 9157 (2008).

[41] See supplementary material at http://link.aps.org/supplemental/10.1103/PhysRevB.81.195404 for the full mass spectra with Al_n^- included, and the geometries of all even electron clusters from $CuAl_n^-$ $n=12-20$, and projected density of states for $CuAl_{22}^-$.